European Journal of Cancer 245 (2026) 116945

Contents lists available at ScienceDirect

European Journal of Cancer

journal homepage: www.ejcancer.com

Original Research

Plasma infrared molecular fingerprinting for prostate cancer detection: Prospective evidence for a partially PSA-independent signal

Philip Jacob [a,b,1,2], Michael Chaloupka [c,2], Tarek Eissa [a,b], Joseph Rebel [a], Jacqueline Aschauer [a], Carola Pfundmeier [a,c], Sabine Witzens [a,c], Isabel Brinkmann [c], Lennert Eismann [c], Nikolaos Pyrgidis [c], Ferenc Krausz [a,b], Frank Fleischmann [a,b], Christian Stief [c,3], Mihaela Žigman [a,b,*,3]

[a] Ludwig-Maximilians-Universität München (LMU), Chair of Experimental Physics - Laser Physics, Am Coulombwall 1, Garching 85748, Germany
[b] Max Planck Institute of Quantum Optics (MPQ), Laboratory for Attosecond Physics, Hans-Kopfermann-Straße 1, Garching 85748, Germany
[c] University Hospital of the Ludwig-Maximilians-Universität München (LMU), Department of Urology, Marchioninistraße 15, München 81377, Germany

ARTICLE INFO

Keywords:
Prostate cancer
Prostate-specific antigen
Infrared molecular fingerprinting
Plasma diagnostics
Molecular spectroscopy

ABSTRACT

Background: Prostate-specific antigen (PSA) testing has limited specificity, particularly at intermediate concentrations, contributing to diagnostic uncertainty in prostate cancer (PCa). Infrared molecular fingerprinting (IMF) provides a rapid plasma-based readout of systemic biochemical variation and may capture PCa-associated molecular information not fully reflected by PSA.
Methods: In the prospective *Lasers4Life* study, plasma from 2024 men was analysed, including 1012 treatment-naïve PCa patients, 752 men with benign prostatic hyperplasia (BPH), and 260 asymptomatic controls. Classification models were evaluated using cross-validation and, for PCa-versus-BPH discrimination, temporally independent held-out testing. Performance was quantified by receiver operating characteristic area under the curve (ROC AUC) and examined across PSA strata, comorbidities, and medications.
Results: IMF discriminated PCa from asymptomatic controls more strongly than from BPH, with cross-validated AUCs of 0.79 ± 0.08 and 0.67 ± 0.04, respectively. In an exploratory age- and PSA-matched subset of men with PSA below 12 ng/mL, comprising 200 PCa and 200 BPH cases, IMF showed higher discrimination than PSA alone, although performance remained modest (AUC 0.63 vs 0.56; $p < 1 \times 10^{-4}$). Most examined comorbidities and medications did not substantially alter IMF performance, although prostatitis reduced discrimination.
Conclusions: Plasma IMF detected PCa-associated variation in a pre-treatment diagnostic setting, including information partly independent of PSA. However, discrimination was modest in the clinically relevant PCa-versus-BPH comparison and did not exceed PSA in the overall cohort. These findings support further evaluation of IMF as an adjunctive molecular-profiling approach, requiring independent multicentre validation, clinically significant PCa endpoints, and demonstration of additive value within established diagnostic pathways.

Introduction

Prostate cancer (PCa) is the second most commonly diagnosed cancer in men worldwide [1]. A central challenge in PCa diagnostics is to identify clinically significant disease while avoiding unnecessary biopsies, overdiagnosis, and overtreatment of indolent tumours. Accurate early detection and risk stratification are therefore essential to guide biopsy decisions, treatment selection, and surveillance, while limiting treatment-related morbidity.

Current diagnostic pathways for PCa still have several limitations. Histopathological assessment using Gleason grading and grade group assignment remains the basis of risk classification, but depends on

* Correspondence to: Chair of Experimental Physics - Laser Physics, Ludwig-Maximilians-Universität München (LMU), Am Coulombwall 1, Garching 85748, Germany.
E-mail address: mihaela.zigman@mpq.mpg.de (M. Žigman).
[1] Present address: Eindhoven University of Technology, Department of Applied Physics and Science Education, 5600 MB Eindhoven, The Netherlands
[2] These authors contributed equally to the work.
[3] These authors jointly supervised the work.

https://doi.org/10.1016/j.ejca.2026.116945

Available online 10 July 2026
0959-8049/© 2026 The Authors. Published by Elsevier Ltd. This is an open access article under the CC BY license (http://creativecommons.org/licenses/by/4.0/).

prostate tissue biopsy and is vulnerable to sampling error, tumour heterogeneity, and inter-observer variation [2]. PSA testing is widely used for initial risk assessment, yet lacks specificity and has limited ability to distinguish indolent from clinically significant PCa [3]. As a result, PSA-based pathways can lead to unnecessary biopsies and overdiagnosis, while a proportion of men with clinically significant PCa have PSA concentrations below commonly used biopsy thresholds [4-6]. Long-term screening data indicate a modest reduction in PCa mortality, which must be weighed against diagnostic and treatment-related harms [7,8]. These limitations support the development of minimally invasive approaches that can complement PSA and imaging, improve selection for biopsy, and refine risk stratification [9,10].

Contemporary PCa diagnostic pathways increasingly incorporate pre-biopsy multiparametric MRI (mpMRI) [11,12]. Blood-based and urine-based biomarker tests (e.g., kallikrein panels, urinary RNA markers) have also been evaluated as adjuncts to PSA for risk stratification [13-17]. Most such approaches, however, rely on predefined molecular targets or selected analyte panels. In contrast, infrared molecular fingerprinting (IMF) provides an untargeted, high-throughput biochemical readout of plasma or serum. As a systems-level adjunct - rather than a replacement for PSA, mpMRI, or established risk models - its possible value within established PCa diagnostic pathways remains to be defined.

IMF using Fourier transform infrared (FTIR) spectroscopy provides a label-free, rapid, and high-throughput method for characterising the biochemical composition of blood-based matrices [18]. FTIR spectra capture composite information from major biomolecular classes, including proteins, lipids, carbohydrates, and metabolites, using microlitre-scale sample volumes. Combined with machine learning, IMF has shown promise for detecting and stratifying common non-communicable diseases [19]. In PCa, early pilot studies reported moderate classification of PCa patients and reference individuals [20,21] and analyses of PCa tumour tissue biopsies demonstrated that FTIR spectra capture tumour-associated and progression-related infrared signatures [22]. However, prior studies have generally been limited by small sample sizes (<100 individuals per group) [23], limited validation, and susceptibility to dataset-specific bias and overfitting. Direct benchmarking against PSA-based models in the same study population has also been limited, leaving unclear whether plasma IMF profiles PCa-associated information beyond PSA.

In this prospective study of 2024 men, we evaluated plasma IMF as a minimally invasive adjunct for prostate cancer detection and risk assessment. We tested whether IMF profiles distinguish PCa from asymptomatic controls and benign prostatic hyperplasia (BPH), and whether they contain PCa-associated biochemical information not reflected by PSA alone. Machine learning models were developed using matched groups and cross-validation, and evaluated on a temporally separated, independently enrolled, and independently measured test-set of individuals. We further assessed the influence of common comorbidities and medication use, and examined performance in clinically relevant subgroups, specifically focusing on men with equivocal PSA levels. Together, these analyses were designed to assess whether plasma IMF provides reproducible molecular information that may complement established prostate cancer diagnostic pathways.

Materials and methods

Clinical study design

The prospective observational study *"Lasers4Life"* was approved by the LMU Munich Ethics Committee (#17–182 and #19–574 fed), conducted in accordance with the ICH-GCP guidelines and the Declaration of Helsinki, and registered in the German Clinical Trials Register (DRKS: ID DRKS00013217 and DRKS00019844). All participants provided written informed consent.

Subject recruitment, study enrolment, and venipuncture were performed at the Department of Urology, LMU University Hospital, Munich, Germany. Men with clinical suspicion of prostate cancer were prospectively enrolled. Clinical suspicion was defined as an elevated or rising PSA value, an abnormal finding on digital rectal examination, or both, consistent with standard urology referral criteria. Peripheral blood samples were collected prior to histopathological diagnosis and processed according to established standard operating procedures [21,24]. Following clinical assessment and, for the PCa and BPH groups, histopathologic evaluation, participants were classified into three groups: men with prostate cancer (PCa), men with benign prostatic hyperplasia (BPH), and asymptomatic reference (AR) individuals. The AR group comprised men without urological symptoms and without clinical suspicion of prostate disease who attended the clinic for unrelated reasons. The BPH group comprised men with lower urinary tract symptoms who received a BPH diagnosis following histopathological evaluation; it is acknowledged that a proportion of BPH-classified participants may harbour occult prostate malignancy undetected at the time of enrolment, which may conservatively attenuate the observed PCA-versus-BPH discrimination.

Samples were organized into two independent cohorts from temporally distinct and non-overlapping enrolment periods: *sample set 1* (enrolment and venipuncture from 2017 to 2021), and *sample set 2* (enrolment and venipuncture from 2023 to 2024). Phenotype distributions for the two cohorts are shown in Supplementary Figure 1 (panels A - C and A'- C', respectively). Enrolment, venipuncture, plasma processing, and sample handling followed the same standard operating procedures across both cohorts [21,24].

Analyses included only treatment-naïve participants with pathologically confirmed PCa and no history of malignant disease within the preceding two years. The exclusion criteria were as follows: age < 18 years; history of any cancer or cancer therapy during the last two years; HIV, HCV or HBV positivity; acute infection; autoimmune disease; any contraindication to venipuncture; or classification as a vulnerable individual.

Blood sample collection and pre-analytical procedures

Venous blood was collected using 21 G Safety-Multifly needles (Sarstedt) into 4.9 mL or 7.5 mL EDTA plasma monovettes (Sarstedt), centrifuged within 3 h at 2000 × g for 10 min at 20 °C. Plasma supernatants were aliquoted and stored at −80 °C. To standardise pre-analytical handling, all samples were thawed once, re-aliquoted, and re-frozen at −80 °C, ensuring that each sample underwent exactly two freeze–thaw cycles before spectroscopic analysis. Immediately before measurements, aliquots were thawed at room temperature, mixed for 30 s at 2000 rpm, and briefly centrifuged.

Infrared fingerprinting measurement

Infrared molecular fingerprinting (IMF) was performed using Fourier transform infrared (FTIR) spectroscopy, as previously described for blood-based molecular fingerprinting [25]. Infrared light is resonantly absorbed as molecules are excited into higher vibrational energy levels. As the energy levels are unique to the constituent molecules, the infrared (IR) spectrum serves as an "infrared molecular fingerprint" that carries quantitative information on the sample's molecular composition [25].

An automated FTIR spectrometer (CLADE™ MIRA-Analyzer, Esslingen, Germany) was used to perform liquid-phase spectroscopic measurements with a flow-through transmission cuvette (CaF_2, 8 μm path length). The spectra were acquired with a resolution of 4 cm^{-1} in a spectral range between 950 cm^{-1} and 3050 cm^{-1}. Each plasma sample measurement was followed by a reference water measurement to calibrate the infrared absorption spectra, leading to a total measurement time of 3.5 min per sample.

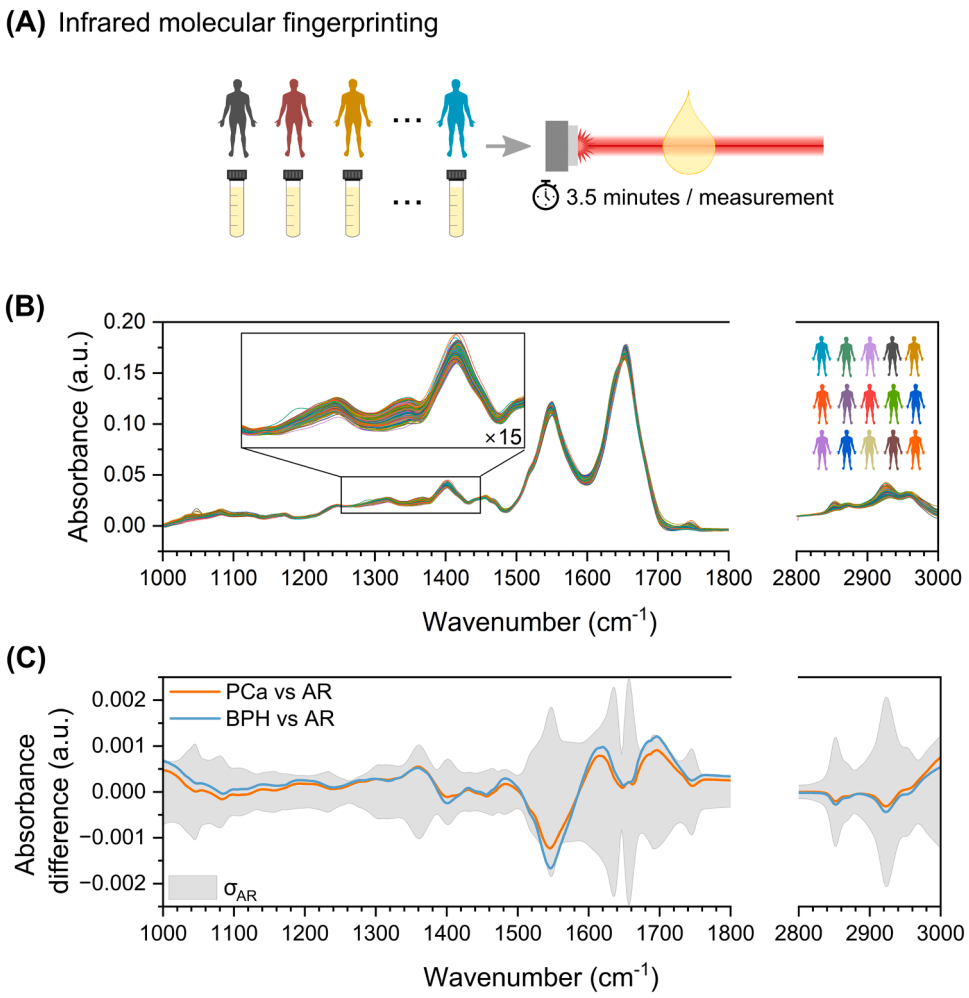

Fig. 1. Infrared molecular fingerprinting scheme. (A) Plasma samples are extracted from the venous blood drawn from study participants. The samples are measured using an FTIR spectrometer to obtain an absorption spectrum. (B) Absorption spectra of all 2024 study participants (normalized) plotted as a function of wavenumber. The inset zooms into a section of the spectra spanning wavenumbers between 1250 and 1450 cm^{-1}. (C) Mean difference in the absorbance between the following pairs of sub-groups: (i) PCa-versus-AR individuals in orange, and (ii) BPH-versus-AR in light blue. The shaded region represents the standard deviation within the AR group (σ_{AR}). PCa: Prostate Cancer, AR: Asymptomatic references, BPH: Benign Prostatic Hyperplasia

Data pre-processing

A total of 18 outlier spectra were removed using the Local Outlier Factor method implemented in Scikit-Learn [26] (v. 1.1.3). Outlier detection was performed on spectral data without diagnostic label annotation. The removed outlier spectra are not included in the cohort description in Table 1.

Water subtraction for each spectroscopic measurement was performed using the corresponding water reference measurement. To correct for potential over-subtraction of the water spectrum, an established approach was applied [27]. A pre-recorded water spectrum was scaled and subtracted so as to obtain a flat baseline in the wavenumber region from 2000 cm^{-1} to 2300 cm^{-1}, where there are no other known significant absorbing molecules in blood plasma apart from water. Each spectrum vector was normalized through division by the Euclidean norm.

Matching of case and control groups

Age, body mass index (BMI), and comorbidity burden were considered potential sources of bias for the classification analysis. To mitigate confounding, case and control groups were matched for age and BMI before training classification models, and performance was additionally evaluated in comorbidity-stratified subgroups. To minimise measurement-related bias, samples from different subgroups were analysed in a randomised order during FTIR measurements. Models were trained on the matched training cohort and evaluated on an independent held-out test set to assess generalisability and reduce the risk of overfitting.

Only male individuals were included. Case and control groups were matched for age and BMI using optimal pair matching based on Mahalanobis distance within propensity score calipers [28] in R (v 3.5.1). Samples from different subgroups were measured in randomized order. Group sizes and the distribution of the matched parameters for each binary classification model are reported in Supplementary Tables 1–3. Matching was performed prior to model training.

Comorbidity and medication subgroup analyses

Subgroup analyses focused on four common, biologically relevant comorbidities: hypertension, type 2 diabetes, prostatitis, and impaired kidney function (defined as eGFR <60 mL/min). These conditions were selected because they were prevalent in the study cohort (Table 1) and could plausibly alter systemic plasma composition, with potential effects on infrared spectral profiles [19]. The medications analysed (finasteride, tamsulosin, dutasteride, silodosin, and alfuzosin) represent commonly used pharmacological treatments for BPH and were assessed because their use was enriched in the BPH comparator group.

Table 1
Overall cohort characteristics across 2024 study participants including categorization into the main physiological groups, distribution of anthropometric factors, measured blood parameters, and comorbidities.

Cohort characteristics (N = 2024)					
Category	**N**	**Age (y)**	**BMI (kg/m^2)**		
Prostate cancer	1012	67.6 ± 8.2	26.8 ± 3.8		
Benign prostatic hyperplasia	752	69.7 ± 8.9	26.4 ± 3.7		
Asymptomatic reference	260	65.7 ± 10.7	27.1 ± 5.0		
Anthropometric parameters	**Mean**	**Std. Dev.**	**Min**	**Max**	**Median**
Age (y)	68.1	8.9	44	90	68
Body height (cm)	178	14	154	202	178
Body weight (kg)	84.4	13.6	48	235	83
BMI (kg/m^2)	26.7	4	15.5	74.2	26.2
BMI categories	**Underweight (<18.5)**	**Normal (18.5 – 25)**		**Overweight (>25)**	
N	9	742		1273	
Smoking status	**Never smoker**	**Former smoker**		**Active smoker**	
N	1101	721		202	
Blood parameters	**Mean**	**Std. Dev.**	**Min**	**Max**	**Median**
Leukocytes(/nL)	7.1	2.1	0.4	25.6	6.8
Haemoglobin(g/dL)	14.7	1.4	7	18.7	14.8
Thrombocytes(/nL)	240	72	65	1358	231
eGFR (mL/min)	78.7	17.1	10	115	82
Comorbidities	**Positive**	**Negative**		**Unspecified**	
Hypertension	1007	1005		12	
Type 2 Diabetes	259	1734		31	
Prostatitis	505	1516		3	
Thyroid disease	297	1693		34	
eGFR < = 60 mL/min	235	1602		187	
PSA > 4 ng/mL	1300	514		210	

Prostate cancer patients (N = 1012)							
Gleason score	**6**	**7a**	**7b**	**8**	**9**	**10**	**Unspecified**
N	213	367	210	90	118	4	10
N with PSA < = 4 ng/mL	54	31	2	3	10	0	1
Average PSA (ng/mL)	9.9	10.7	18.7	21.4	34.3	36.5	50.8
Prostate tumour volume percent (%)	**< = 10**	**11 – 25**	**26 – 50**	**51 – 75**	**> 75**		**Unspecified**
N	282	343	192	44	20		131
Tumour T-stage	**pT1**	**pT2**	**pT3**	**pT4**			**Unspecified**
N	39	518	327	3			125

Continuous variables are summarized by the mean, standard deviation (std. dev.), minimum (min), maximum (max), and median; numbers of individuals per group (N) are shown as counts. The bottom panels correspond to the prostate cancer group consisting of 1012 participants. Gleason score, tumour T-stage, and tumour volume percentage were all assigned based on pathological analysis after prostatectomy. BMI: Body Mass Index, eGFR: Estimated Glomerular Filtration Rate, PSA: Prostate-Specific Antigen.

Handling of missing data

Two individuals had missing values for BMI and were excluded from the study. For the comparative analysis between infrared fingerprinting and PSA testing, individuals with missing PSA values were excluded from the analysis to ensure paired availability of both tests. This reduced the BPH cohort and the matched PCa group size by 15 each (from 752 to 737).

Statistical models

Binary classification models based on logistic regression were developed using the Scikit-learn [26] (v. 1.1.3) open-source machine learning framework in Python (v. 3.9.12). Model development and performance estimation were carried out using a nested cross-validation approach in all cases except one, in which a held-out test set was utilized (represented by the black curve in Fig. 2B). Results were visualized using receiver operating characteristic (ROC) curves and the classification efficiency was quantified by the area under the ROC curve (AUC). In the cases where cross-validation was performed, the mean and standard deviation of the AUCs were reported. For selective cross-validation analyses across comorbidity-specific subgroups, training in each cross-validation fold was performed without further selection criteria, while validation was performed separately for subsets of individuals who are either positive or negative for the specified comorbidity or medication intake.

Results

Infrared molecular fingerprinting of blood plasma

The study included 2024 participants, with cohort characteristics summarized in Table 1. Plasma was analysed by infrared molecular fingerprinting (Fig. 1A), generating an infrared absorption spectrum (absorbance versus wavenumber) per individual (Fig. 1B). Differential absorbance profiles ("differential fingerprints") were computed by subtracting the mean normalized spectrum of matched asymptomatic reference controls (AR; individuals without prostate-related symptoms) from the mean normalized spectra of the case groups: PCa (orange) and BPH (light blue), as shown in Fig. 1C. The grey shaded area represents the standard deviation of the AR group. Group-level differences motivated supervised classification analyses.

Prostate cancer detection

We linked infrared molecular fingerprints to the participants' clinical data to evaluate their ability to detect PCa. Fig. 2A shows ROC curves for binary classifiers distinguishing asymptomatic references (AR) from PCa (orange) and BPH (cyan). All 260 AR control individuals and 260 matched PCa case individuals were used in both comparisons (Supplementary Table 1). Fig. 2A' summarizes the mean AUC values with standard deviations. Cross-validated performance was high for the BPH-versus-AR classifier (AUC = 0.87 ± 0.04), and moderate for the

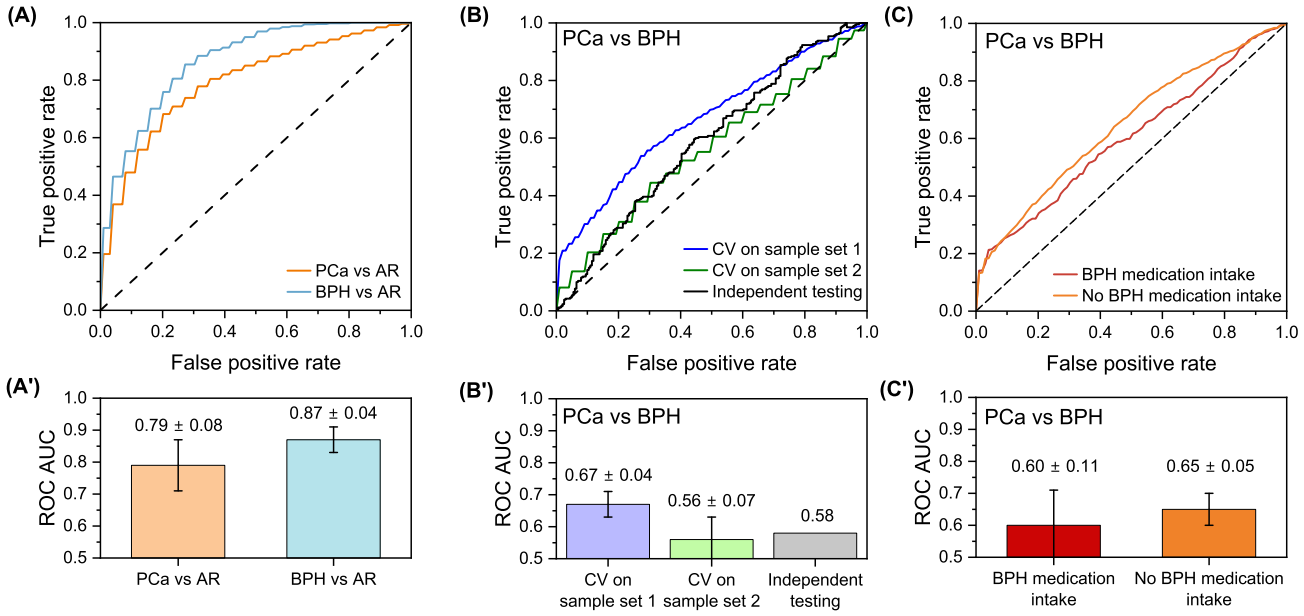

Fig. 2. Detection of prostate cancer and benign prostatic hyperplasia from blood plasma infrared molecular fingerprints. (A) ROC curves for binary classification of asymptomatic reference (AR) individuals from individuals with PCa (orange) and BPH (cyan) on performing 10-fold cross-validation with 5 repetitions in sample set 1. (A') Area under the ROC curves (ROC AUC) shown in A. (B) ROC curves for binary classification between PCa patients and BPH references on performing (i) cross-validation within sample set 1 shown in blue, (ii) cross-validation within sample set 2 shown in green, and (iii) model training on sample set 1 and testing on sample set 2 shown in black. (B') Area under the ROC curves displayed in B. (C) ROC curves obtained with the PCa-versus-BPH binary classification model on cross-validating with medication-stratified subsets in the combined cohort. (C') Area under the ROC curves displayed in C. Predictions were evaluated on held-out cross-validation folds or, where indicated, on the temporally independent test cohort. PCa: Prostate Cancer, AR: Asymptomatic references, BPH: Benign Prostatic Hyperplasia, ROC: Receiver Operating Characteristic, AUC: Area Under the Curve, CV: Cross-Validation.

PCa-versus-AR classifier (AUC = 0.79 ± 0.08). Because AR comparisons are less clinically stringent, we next assessed PCa-versus-BPH discrimination.

In the clinically more stringent PCa-versus-BPH comparison, separate binary classification models in each cohort were trained and tested on the temporally separated cohort. Figure panels 2B and 2B' display three evaluations: (i) within-cohort cross-validation within sample set 1 (blue), (ii) within-cohort cross-validation within sample set 2 (green), and (iii) model training on sample set 1 with independent testing on sample set 2 (black). Cross-validation AUC was higher in sample set 1 (ROC AUC of 0.67 ± 0.04) than in sample set 2 (0.56 ± 0.07). Gleason score and tumour stage distributions were similar across cohorts (Supplementary Figure 1).

When a model was trained on sample set 1 and tested on sample set 2, an AUC of 0.58 was achieved, indicating limited discrimination in the independent temporal validation cohort. This is analogous to the within-cohort performance in sample set 2, suggesting limited discriminative signal within that cohort. Consistent with the aforementioned observations, the model that was trained on sample set 2, which demonstrated comparatively limited cross-validation performance, also exhibited limited performance when tested on sample set 1 (Supplementary Figure 2A). Minor shifts in age distribution or other unmeasured confounding variables may have contributed to these differences. Altogether, PCa-versus-BPH generalization was modest.

Impact of comorbid conditions and medication intake

Chronic conditions may influence infrared molecular fingerprints and obscure PCa-associated signals. We evaluated whether four prevalent comorbidities - hypertension, type 2 diabetes, prostatitis, and reduced kidney function (defined as eGFR <60 mL/min) - altered binary PCa-versus-BPH classification.

Using 10-fold selective cross-validation in 752 PCa patients and 752 matched BPH individuals (Supplementary Table 2), we assessed whether each comorbidity altered discrimination. Similar AUCs in comorbidity-positive and -negative validation subsets suggested limited interference with PCa classification (Supplementary Figure 2B). The ROC AUC for PCa-versus-BPH showed a slight decrease when validated on the prostatitis-positive subgroup compared to the prostatitis-negative subgroup (0.60 ± 0.09 and 0.66 ± 0.04, respectively; paired *t*-test, $p < 0.001$; Supplementary Figure 2B). We attribute this decrease to the fact that prostatitis induces inflammatory changes that may alter plasma molecular makeup in ways that partially overlap with or obscure cancer-associated spectral features.

We further investigated whether medications commonly prescribed for BPH could influence classification performance. Analysed medications included finasteride, tamsulosin, dutasteride, silodosin, alfuzosin, and their combinations. Individuals receiving BPH medication showed a marginally lower ROC AUC (0.60 ± 0.11) than those without BPH medication intake (0.65 ± 0.05). Yet, this difference was not statistically significant (Figure panels 2C, 2C'). Overall, prostatitis modestly reduced IMF discrimination, whereas BPH medication showed only a non-significant trend toward lower AUC.

Comparisons of infrared molecular fingerprinting to the diagnostic efficacy of PSA

To benchmark IMF against standard clinical testing, we evaluated PSA, which was available for nearly all participants. Fig. 3A displays the PSA distributions for 737 PCa patients and 737 age- and BMI-matched individuals with BPH (Supplementary Table 3), with median PSA concentrations of 8.5 ng/mL and 4.4 ng/mL, respectively.

We compared models using PSA alone, infrared fingerprints alone, or both. The corresponding ROC curves are shown in Fig. 3B, and AUC values are summarized in Fig. 3C. In the overall cohort, the PSA-only classifier outperformed IMF, with a ROC AUC of 0.73 ± 0.05

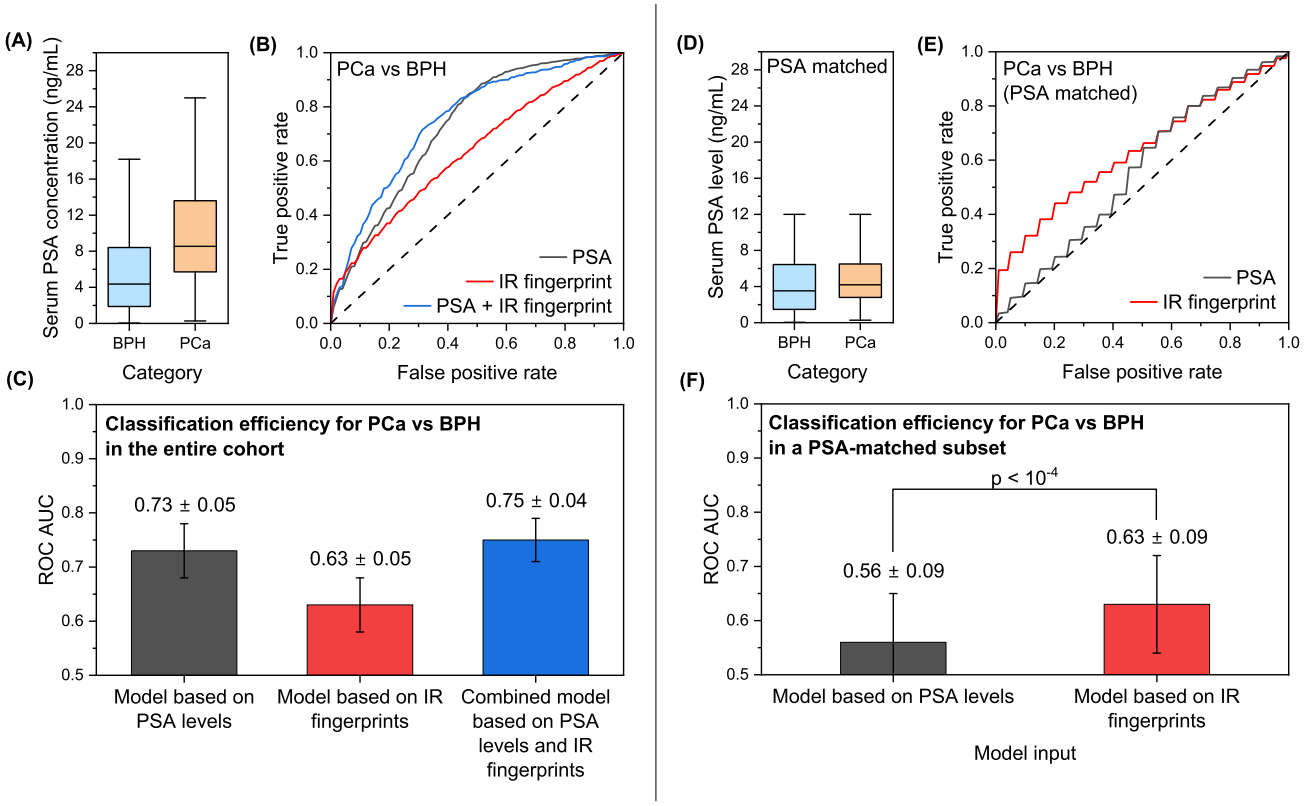

Fig. 3. Detection of PCa from infrared (IR) fingerprints as compared to prostate-specific antigen (PSA) testing. (A) Distribution of total serum PSA concentrations in the BPH and PCa groups. (B) Mean ROC curves obtained with the binary classifier model using (i) prostate-specific antigen concentration values (grey), (ii) IR fingerprint data (red), and (iii) a combination of both PSA and IR fingerprints, on cross-validating in the combined cohort. (C) Mean and standard deviation of ROC AUCs for the cases displayed in (B). (D) Distribution of serum PSA in subsets of the BPH and PCa groups containing 200 individuals each with matched PSA. (E) ROC curves corresponding to BPH-versus-PCa classification models trained on (i) serum PSA values (grey), and (ii) IR fingerprinting data (red) from the selected subsets with matched PSA. (F) Mean and standard deviation of ROC AUCs for the analyses displayed in (E). PCa: Prostate Cancer, BPH: Benign Prostatic Hyperplasia, PSA: Prostate-Specific Antigen, IR: Infrared, ROC: Receiver Operating Characteristic, AUC: Area Under the Curve.

compared to 0.64 ± 0.04 for the infrared fingerprint classifier. These findings indicate that IMF did not outperform PSA in the overall cohort, although its partly distinct signal may still be relevant in selected PSA-overlapping settings. Combining PSA and IMF yielded a slightly higher cross-validation ROC AUC of 0.75 ± 0.04. The optimum weight values of 0.88 for the PSA-based prediction, and 0.12 for the infrared fingerprint-based prediction were obtained by performing an inner cross-validation on each split of the (outer) cross-validation. The combined model thus relied predominantly on PSA.

To assess IMF in a setting where the PSA discrimination is limited, we randomly selected 200 PCa patients with PSA below 12 ng/mL. This threshold reduced the dominance of high-PSA cases, in which the probability of malignancy is substantially increased, while retaining sufficient sample size for matched analysis. We selected 200 age- and PSA-matched BPH individuals for comparison (Supplementary Table 3). This was an exploratory PSA-matched analysis.

The PSA distributions for these subsets are displayed in Fig. 3D, with median PSA values of 4.2 ng/mL (PCa patients) and 3.5 ng/mL (BPH references). Fig. 3E presents the ROC curves for models using PSA only (grey) or the infrared fingerprints only (red) as the input, with AUCs summarized in Fig. 3F. In this PSA-matched setting, infrared fingerprinting showed higher discrimination than PSA alone, achieving an AUC of 0.63 ± 0.09 compared to 0.56 ± 0.09 for PSA ($p < 10^{-4}$). Although the absolute discrimination remained moderate, this improvement indicates that infrared fingerprints capture diagnostic information not represented by PSA concentration alone.

Together, these results indicate that infrared molecular profiles capture PCa-associated biological variation partly independent of PSA. IMF did not surpass PSA in the overall cohort, but demonstrated higher discrimination in the exploratory PSA-matched analysis. This should not be interpreted as broad diagnostic superiority.

Discussion

Blood-based infrared molecular fingerprinting (IMF) has shown potential for several malignancies [20,21,29,30,31], including prostate cancer (PCa) [21,23], as well as non-communicable diseases [19,32]. Infrared microspectroscopy of prostate tissue sections has also distinguished malignant from benign tissue [33]. However, the clinical settings in which IMF of blood matrices may address unmet diagnostic needs remained insufficiently defined.

In this prospective cohort of more than 2000 individuals, including over 1000 men with PCa, plasma-based IMF captured PCa-associated molecular variation, consistent with previous findings [21,30]. Because participants were enrolled and sampled before diagnosis and treatment initiation, the study reflects a clinically relevant pre-treatment diagnostic setting. These findings support the biological plausibility of plasma IMF as a source of PCa-associated molecular information. However, modest discrimination in the PCa-versus-BPH comparison indicates that, although plasma IMF contains PCa-associated molecular information, IMF should not be interpreted as a stand-alone diagnostic test at this stage. Rather, its potential value lies in further development as an adjunctive molecular-profiling approach within established diagnostic pathways.

Discrimination was stronger for PCa versus asymptomatic matched controls (AUC 0.79) than for PCa versus BPH (AUC 0.67), likely

reflecting greater biological and clinical overlap between malignant and benign prostatic disease. The PCa-versus-BPH comparison is the more clinically relevant benchmark, as both groups may present with lower urinary tract symptoms and elevated or borderline PSA values. Moreover, men classified as PCa-negative after bladder outlet obstruction surgery (e.g., TURP or HoLEP) may still harbour occult prostate malignancy. Incidental cancers detected in TURP and HoLEP specimens, together with long-term follow-up data, indicate that a subset of patients initially considered as benign are later diagnosed with PCa [34-36]. Occult PCa in the BPH comparator group may therefore have attenuated classification performance, suggesting that the observed discrimination could represent a conservative estimate of IMF signal strength.

Systemic molecular profiling is inherently susceptible to confounding by comorbidities and medication use. Age and body mass index were addressed through matching and are therefore unlikely to have substantially influenced the results. Chronic conditions such as hypertension and type 2 diabetes may influence infrared molecular fingerprints [19]. Other relevant clinical factors in these cohorts included prostatitis and abnormal kidney function. Comorbidity-stratified analyses suggested that most common chronic conditions did not dominate the cancer-associated IMF signatures. Prostatitis was an important exception and was associated with significantly reduced discrimination (AUC 0.60 ± 0.09 in prostatitis-positive versus 0.66 ± 0.04 in prostatitis-negative individuals, $p < 0.001$). This is biologically plausible, as prostatitis involves inflammatory cell infiltration and may introduce inflammation-related variation that overlaps with, or obscures, PCa-associated spectral signatures. Prostatitis should therefore be considered a potential modifier of IMF performance in future clinical studies.

Concomitant medication use represents another potential source of variation in plasma composition. In this study, diagnostic performance was only modestly reduced among participants receiving medication, and exploratory analyses showed no statistically significant association between BPH medication use and IMF performance. These results should be interpreted cautiously, as medication classes may have distinct biological effects that were not fully resolved here. Notably, 5-α-reductase inhibitors, such as finasteride, can lower serum PSA concentrations [37], potentially complicating PSA-based PCa detection. Medication-specific effects on IMF performance therefore require dedicated prospective evaluation.

Several serum [13-15,38] and urine biomarkers [16] have been proposed for PCa detection, yet PSA remains the most widely used test in clinical practice [39]. Ongoing debate regarding the benefit-harm balance of PSA-based screening [40-43] has driven efforts to improve risk-stratification through clinical risk factors [14], biomarkers and MRI-informed strategies [11,12,42]. PSA has limited specificity at the commonly used 4 ng/mL threshold, contributing to false-positive findings and unnecessary biopsies [44], while low PSA does not reliably exclude malignancy. In the prostate cancer prevention trial, PCa was detected on biopsy in 15.2% of men with PSA $\leq$ 4 ng/mL, and 6.6% with PSA $\leq$ 0.5 ng/mL [5]. These limitations provide a rationale for evaluating IMF in clinical contexts where PSA-based discrimination is uncertain.

IMF should therefore not be positioned as a replacement for PSA, MRI, or established risk models. Its more plausible role is as a candidate adjunctive *in vitro* diagnostic modality that may refine molecular risk assessment, particularly in men with equivocal PSA values before biopsy or MRI referral. Any such role must be evaluated within an increasingly sophisticated diagnostic landscape that already includes validated biomarker and imaging strategies, such as kallikrein-based tests, the Stockholm3 model, 4Kscore and MRI-informed pathways [11-14]. Established multi-analyte tools have reported stronger discrimination for clinically significant or high-grade prostate cancer than IMF achieved in the present PCa-versus-BPH analysis. However, these comparisons are indirect because endpoints, study populations, and diagnostic pathways differ.

IMF also differs methodologically from targeted biomarker approaches: Whereas kallikrein-based tools combine predefined protein measurements with clinical variables, IMF captures a broader untargeted composite molecular profile of plasma from a single spectroscopic assay. This broader molecular readout is scientifically attractive, but its clinical relevance will depend on improved discrimination, validation against clinically significant disease, and demonstration of additive value within contemporary risk-stratification pathways. The present results thus position plasma IMF as a scalable source of PCa-associated molecular information that warrants further translational development.

Several limitations should be considered. Firstly, this was a single-centre study, which may limit its generalisability to population-based screening or primary-care settings. Secondly, independent multicentre validation is required prior to clinical translation. Thirdly, the performance in the clinically relevant PCa-versus-BPH comparison was modest, and IMF did not outperform PSA overall. Fourthly, the PSA-matched subgroup analysis was exploratory. The fifth point to consider is that the study evaluated the detection of PCa in general, rather than clinically significant PCa. Finally, occult PCa in the BPH or asymptomatic control groups could not be excluded where systematic diagnostic verification was not performed, and longitudinal follow-up would be needed to address this limitation. These limitations are counter balanced by methodological strengths, including the prospective enrolment, large cohort size, standardised pre-analytical and analytical workflows, randomised measurement order, and temporally separated validation. Collectively, these features support the reliability of the observed biological IMF signal, while defining the evidence required for clinical translation. Advancements in laser-based infrared spectroscopy [45] and automated pre-analytical workflows have the potential to further improve scalability. Although the IMF assay is rapid, high-throughput, and requires only microlitre-scale plasma volumes, clinical adoption will require reproducible performance and demonstrated additive value within established diagnostic pathways.

Conclusions

In this prospective study, plasma IMF detected PCa-associated molecular variation in a pre-treatment diagnostic setting. Diagnostic performance was modest, particularly in the clinically relevant PCa-versus-BPH comparison, and did not exceed PSA in the overall cohort. Exploratory PSA-matched analyses suggest that IMF may capture biochemical information partly independent of PSA, supporting further evaluation as an adjunctive molecular profiling approach in selected diagnostic contexts. Performance was not substantially altered by most examined comorbidities or concomitant medications, although prostatitis modestly reduced discrimination. These findings support further translational development of IMF as an adjunctive molecular-profiling approach, while clinical implementation will require multicentre validation against clinically significant PCa and demonstrated additive value within contemporary PSA-, biomarker-, and MRI-informed pathways.

CRediT authorship contribution statement

Mihaela Žigman: Conceptualization, Funding acquisition, Investigation, Methodology, Project administration, Resources, Supervision, Writing – original draft, Writing – review & editing. **Philip Jacob:** Data curation, Formal analysis, Investigation, Methodology, Validation, Visualization, Writing – original draft, Writing – review & editing. **Michael Chaloupka:** Conceptualization, Investigation, Methodology, Supervision, Writing – review & editing. **Tarek Eissa:** Conceptualization, Formal analysis, Investigation, Methodology, Visualization, Writing – review & editing. **Joseph Rebel:** Investigation, Methodology, Writing – review & editing. **Jacqueline Aschauer:** Data curation, Project administration, Supervision, Writing – review & editing. **Carola Pfundmeier:** Investigation, Methodology, Project administration.

Sabine Witzens: Investigation, Methodology, Project administration, Writing – review & editing. **Isabel Brinkmann:** Investigation, Writing – review & editing. **Lennert Eismann:** Investigation, Writing – review & editing. **Nikolaos Pyrgidis:** Investigation, Writing – review & editing. **Ferenc Krausz:** Conceptualization, Resources, Writing – review & editing. **Frank Fleischmann:** Investigation, Methodology, Supervision, Writing – review & editing. **Christian Stief:** Conceptualization, Funding acquisition, Investigation, Methodology, Supervision, Writing – original draft, Writing – review & editing.

Consent for publication

All authors consent to the publication of this manuscript.

Ethics approval and consent to participate

Research described in the manuscript was conducted with written informed consent and ethics approval (LMU protocols #17–182 and #19–574 fed) and is registered under the German Clinical Trials Register (DRKS00013217; DRKS00019844).

Funding

This work was supported by the Centre for Advanced Laser Applications (CALA) at LMU Munich and the German Federal Ministry of Research, Technology and Space (BMFTR) through the *CASCADE-IR* project under the *DataXperiment* funding call.

Declaration of Competing Interest

The authors declare that they have no known competing financial interests or personal relationships that could have appeared to influence the work reported in this paper.

Acknowledgements

We gratefully acknowledge the contributions of the many individuals who volunteered to participate in this clinical study. We thank Daniel Meyer and Viola Zóka for their technical support, and we thank Dr. Julia Meyer, Dr. Bianca Hoefelschweiger for their organizational support.

Appendix A. Supporting information

Supplementary data associated with this article can be found in the online version at doi:10.1016/j.ejca.2026.116945.

Data availability

The datasets analysed within the scope of this work cannot be published publicly due to privacy regulations under the General Data Protection Regulation (EU) 2016/679. The raw data include clinical patient information that could potentially compromise subjects' privacy or consent and therefore cannot be shared. The Python code used for analysis is stored in a persistent repository at the Leibniz Supercomputing Center of the Bavarian Academy of Sciences and Humanities (LRZ), and can be made available on reasonable request to the corresponding author.

References

[1] Sandhu S, Moore CM, Chiong E, Beltran H, Bristow RG, Williams SG. Prostate cancer. Lancet 2021;398(10305):1075–90. https://doi.org/10.1016/S0140-6736(21)00950-8.
[2] Mathieu R, Moschini M, Beyer B, et al. Prognostic value of the new Grade Groups in Prostate Cancer: a multi-institutional European validation study. Prostate Cancer Prostatic Dis 2017;20(2):197–202. https://doi.org/10.1038/pcan.2016.66.
[3] Hoffman Richard M. Screening for prostate cancer. New Engl J Med 2011;365(21):2013–9. https://doi.org/10.1056/NEJMcp1103642.
[4] Möller F, Månsson M, Wallström J, Hellström M, Hugosson J, Arnsrud Godtman R. Prostate Cancers in the Prostate-specific Antigen Interval of 1.8–3 ng/mL: Results from the Göteborg-2 Prostate Cancer Screening Trial. Eur Urol 2024;86(2):95–100. https://doi.org/10.1016/j.eururo.2024.01.017.
[5] Thompson Ian M, Pauler Donna K, Goodman Phyllis J, et al. Prevalence of Prostate Cancer among Men with a Prostate-Specific Antigen Level ≤4.0 ng per Milliliter. New Engl J Med 2004;350(22):2239–46. https://doi.org/10.1056/NEJMoa031918.
[6] Leibovici D, Spiess PE, Agarwal PK, et al. Prostate cancer progression in the presence of undetectable or low serum prostate-specific antigen level. Cancer 2007;109(2):198–204. https://doi.org/10.1002/cncr.22372.
[7] Andriole Gerald L, Crawford ED, Grubb Robert L, et al. Mortality Results from a Randomized Prostate-Cancer Screening Trial. New Engl J Med 2009;360(13):1310–9. https://doi.org/10.1056/NEJMoa0810696.
[8] Martin RM, Turner EL, Young GJ, et al. Prostate-Specific Antigen Screening and 15-Year Prostate Cancer Mortality: A Secondary Analysis of the CAP Randomized Clinical Trial. JAMA 2024;331(17):1460–70. https://doi.org/10.1001/jama.2024.4011.
[9] Cornford P, Tilki D, van den Bergh RCN, et al. EAU Guidelines. EAU Annu Congr Madr 2025;86(2):148–63. https://doi.org/10.1016/j.eururo.2024.03.027.
[10] Quinn D, Gross M. Show us a sign: the search for "game changing" prostate cancer biomarkers. Lancet Oncol 2011;12(3):204–6. https://doi.org/10.1016/S1470-2045(11)70003-1.
[11] Björnebo L, Discacciati A, Falagario U, et al. Biomarker vs MRI-Enhanced Strategies for Prostate Cancer Screening: The STHLM3-MRI Randomized Clinical Trial. JAMA Netw Open 2024;7(4):e247131. https://doi.org/10.1001/jamanetworkopen.2024.7131.
[12] Kasivisvanathan V, Rannikko Antti S, Borghi M, et al. MRI-Targeted or Standard Biopsy for Prostate-Cancer Diagnosis. New Engl J Med 2018;378(19):1767–77. https://doi.org/10.1056/NEJMoa1801993.
[13] Bryant RJ, Sjoberg DD, Vickers AJ, et al. Predicting High-Grade Cancer at Ten-Core Prostate Biopsy Using Four Kallikrein Markers Measured in Blood in the ProtecT Study. JNCI J Natl Cancer Inst 2015;107(7). https://doi.org/10.1093/jnci/djv095.
[14] Grönberg H, Adolfsson J, Aly M, et al. Prostate cancer screening in men aged 50-69 years (STHLM3): a prospective population-based diagnostic study. Lancet Oncol 2015;16(16):1667–76. https://doi.org/10.1016/S1470-2045(15)00361-7.
[15] Klein EA, Chait A, Hafron JM, et al. The Single-parameter, Structure-based IsoPSA Assay Demonstrates Improved Diagnostic Accuracy for Detection of Any Prostate Cancer and High-grade Prostate Cancer Compared to a Concentration-based Assay of Total Prostate-specific Antigen: A Preliminary Report. Eur Urol 2017;72(6):942–9. https://doi.org/10.1016/j.eururo.2017.03.025.
[16] Sanda MG, Feng Z, Howard DH, et al. Association Between Combined TMPRSS2: ERG and PCA3 RNA Urinary Testing and Detection of Aggressive Prostate Cancer. JAMA Oncol 2017;3(8):1085–93. https://doi.org/10.1001/jamaoncol.2017.0177.
[17] Van Neste L, Hendriks RJ, Dijkstra S, et al. Detection of High-grade Prostate Cancer Using a Urinary Molecular Biomarker–Based Risk Score. Eur Urol 2016;70(5):740–8. https://doi.org/10.1016/j.eururo.2016.04.012.
[18] Baker MJ, Trevisan J, Bassan P, et al. Using Fourier transform IR spectroscopy to analyze biological materials. Nat Protoc 2014;9(8):1771–91. https://doi.org/10.1038/nprot.2014.110.
[19] Eissa T, Leonardo C, Kepesidis KV, et al. Plasma infrared fingerprinting with machine learning enables single-measurement multi-phenotype health screening. Cell Rep Med 2024;5(7). https://doi.org/10.1016/j.xcrm.2024.101625.
[20] Cameron JM, Sala A, Antoniou G, et al. A spectroscopic liquid biopsy for the earlier detection of multiple cancer types. Br J Cancer 2023;129(10):1658–66. https://doi.org/10.1038/s41416-023-02423-7.
[21] Huber M, Kepesidis KV, Voronina L, et al. Infrared molecular fingerprinting of blood-based liquid biopsies for the detection of cancer. eLife 2021:e68758. https://doi.org/10.7554/eLife.68758.
[22] Kwak JT, Hewitt SM, Sinha S, Bhargava R. Multimodal microscopy for automated histologic analysis of prostate cancer. BMC Cancer 2011;11(1):62. https://doi.org/10.1186/1471-2407-11-62.
[23] Medipally DKR, Cullen D, Untereiner V, et al. Vibrational spectroscopy of liquid biopsies for prostate cancer diagnosis. Ther Adv Med Oncol 2020;12:1758835920918499. https://doi.org/10.1177/1758835920918499.
[24] Huber M, Kepesidis KV, Voronina L, et al. Stability of person-specific blood-based infrared molecular fingerprints opens up prospects for health monitoring. Nat Commun 2021;12(1):1511. https://doi.org/10.1038/s41467-021-21668-5.
[25] Larkin P. Infrared Raman Spectrosc Princ Spectr Interpret 2011. https://doi.org/10.1016/C2010-0-68479-3.
[26] Pedregosa F, Varoquaux G, Gramfort A, et al. Scikit-learn: Machine Learning in Python. J Mach Learn Res 2012;12.
[27] Yang H, Yang S, Kong J, Dong A, Yu S. Obtaining information about protein secondary structures in aqueous solution using Fourier transform IR spectroscopy. Nat Protoc 2015;10(3):382–96. https://doi.org/10.1038/nprot.2015.024.
[28] Rosenbaum P. Design of Observational Studies. Springer; 2010. https://doi.org/10.1007/978-1-4419-1213-8.
[29] Butler HJ, Brennan PM, Cameron JM, et al. Development of high-throughput ATR-FTIR technology for rapid triage of brain cancer. Nat Commun 2019;10(1):4501. https://doi.org/10.1038/s41467-019-12527-5.
[30] Kepesidis KV, Jacob P, Schweinberger W, et al. Electric-Field Molecular Fingerprinting to Probe Cancer. ACS Cent Sci 2025;11(4):560–73. https://doi.org/10.1021/acscentsci.4c02164.

[31] Ollesch J, Theegarten D, Altmayer M, et al. An infrared spectroscopic blood test for non-small cell lung carcinoma and subtyping into pulmonary squamous cell carcinoma or adenocarcinoma. Biomed Spectrosc Imaging 2016;5:129–44. https://doi.org/10.3233/BSI-160144.
[32] Paraskevaidi M, Morais CLM, Lima KMG, et al. Differential diagnosis of Alzheimer's disease using spectrochemical analysis of blood. Proc Natl Acad Sci 2017;114(38):E7929–38. https://doi.org/10.1073/pnas.1701517114.
[33] Ferguson D., Sachdeva A., Hart C., 2025. Identification of at-risk prostate cancer patients using Fourier transform infrared spectroscopy and machine learning. 2025:9. https://doi.org/10.1117/12.3048498.
[34] Hilscher M, Røder A, Helgstrand JT, et al. Risk of prostate cancer and death after benign transurethral resection of the prostate—A 20-year population-based analysis. Cancer 2022;128(20):3674–80. https://doi.org/10.1002/cncr.34407.
[35] Klein C, Marquette T, Capon G, et al. Incidental prostate cancer after holmium laser enucleation of the prostate: incidence and predictive factors for clinical progression. Int J Clin Oncol 2022;27(6):1077–83. https://doi.org/10.1007/s10147-022-02156-2.
[36] Pursnani S, Manivasagam SS, Mohr E, et al. Hidden findings: How often does Holmium laser enucleation of the prostate (HoLEP) uncover prostate cancer? Int Urol Nephrol 2025. https://doi.org/10.1007/s11255-025-04769-8.
[37] Etzioni RD, Howlader N, Shaw PA, et al. Long-term effects of finasteride on prostate specific antigen levels: results from the prostate cancer prevention trial. J Urol 2005;174(3):877–81. https://doi.org/10.1097/01.ju.0000169255.64518.fb.
[38] Vickers AJ, Cronin AM, Aus G, et al. A panel of kallikrein markers can reduce unnecessary biopsy for prostate cancer: data from the European Randomized Study of Prostate Cancer Screening in Göteborg, Sweden. BMC Med 2008;6(1):19. https://doi.org/10.1186/1741-7015-6-19.
[39] Schafer EJ, Laversanne M, Sung H, et al. Recent Patterns and Trends in Global Prostate Cancer Incidence and Mortality: An Update. Eur Urol 2025;87(3):302–13. https://doi.org/10.1016/j.eururo.2024.11.013.
[40] USPSTF. Screening for Prostate Cancer: US Preventive Services Task Force Recommendation Statement. JAMA 2018;319(18):1901–13. https://doi.org/10.1001/jama.2018.3710.
[41] Heijnsdijk EAM, Gulati R, Tsodikov A, et al. Lifetime Benefits and Harms of Prostate-Specific Antigen–Based Risk-Stratified Screening for Prostate Cancer. JNCI Journal National Cancer Institute 2020;112(10):1013–20. https://doi.org/10.1093/jnci/djaa001.
[42] Pinsky Paul F, Parnes H. Screening for Prostate Cancer. New Engl J Med 2023;388(15):1405–14. https://doi.org/10.1056/NEJMcp2209151.
[43] Vertosick EA, Vickers A, Dahlin A, et al. Prostate-specific antigen levels at age 60 years and lifetime risk of lethal prostate cancer. JNCI Journal National Cancer Institute 2025. https://doi.org/10.1093/jnci/djaf271.
[44] Kilpeläinen TP, Tammela TLJ, Roobol M, et al. False-positive screening results in the European randomized study of screening for prostate cancer. Eur J Cancer 2011;47(18):2698–705. https://doi.org/10.1016/j.ejca.2011.06.055.
[45] Schwaighofer A, Montemurro M, Freitag S, Kristament C, Culzoni MJ, Lendl B. Beyond Fourier Transform Infrared Spectroscopy: External Cavity Quantum Cascade Laser-Based Mid-infrared Transmission Spectroscopy of Proteins in the Amide I and Amide II Region. Anal Chem 2018;90(11):7072–9. https://doi.org/10.1021/acs.analchem.8b01632.